

## Magnetotransport properties of $\text{La}_{0.6}\text{Pb}_{0.4}\text{MnO}_{3-\delta}$ and $\text{Nd}_{0.6}(\text{Sr}_{0.7}\text{Pb}_{0.3})_{0.4}\text{MnO}_{3-\delta}$ single crystals

Y. X. Jia, Li Lu, K. Khazeni, Vincent H. Crespi, A. Zettl, and Marvin L. Cohen

*Department of Physics, University of California at Berkeley, Berkeley, California 94720*  
*and Materials Sciences Division, Lawrence Berkeley Laboratory, Berkeley, California 94720*

(Received 11 May 1995)

Magnetotransport measurements of high-quality single crystals of  $\text{La}_{0.6}\text{Pb}_{0.4}\text{MnO}_{3-\delta}$  and  $\text{Nd}_{0.6}(\text{Sr}_{0.7}\text{Pb}_{0.3})_{0.4}\text{MnO}_{3-\delta}$  show a close relationship between giant magnetoresistance and the ferromagnetic ordering transition in these materials. In contrast to results for thin film and polycrystalline materials, magnetoresistance of these single crystals vanishes as  $T \rightarrow 0$ . A two-component polaron model provides a possible framework for the interpretation of the previously unexplained variation in the functional form of  $\rho(H)$  above and below the Curie temperature.

The recent discovery of giant magnetoresistance (GMR) in perovskite manganites such as  $\text{Nd}_{1-x}\text{M}_x\text{MnO}_3$  [ $M=\text{Pb}$ ,<sup>1</sup>  $M=\text{Sr}$  (Ref. 2)] and  $\text{La}_{1-x}\text{M}_x\text{MnO}_3$  [ $M=\text{Ba}$ ,<sup>3</sup>  $\text{Sr}$ ,<sup>4</sup>  $\text{Ca}$ ,<sup>5,6</sup> or  $\text{Pb}$  (Ref. 7)] and in particular the observation of so-called "colossal" magnetoresistance in  $\text{La}_{1-x}\text{Ca}_x\text{MnO}_3$  (Ref. 5) and single-crystal  $\text{Nd}_{1-x}\text{Pb}_x\text{MnO}_3$ ,<sup>1</sup> has sparked renewed interest in these long-known materials<sup>8-11</sup> with an eye towards both an understanding of the mechanism and application of GMR in magnetic devices such as read and/or write heads for magnetic disk drives. The general manganite perovskite formula unit of  $L_{1-x}M_x\text{MnO}_3$  ( $L$ =lanthanide,  $M$ =alkaline earth or lead) contains  $L$  and/or  $M$  ions at the corners of a simple cubic cell, with the smaller Mn ions at the cube centers and the oxygen ions located at the face centers. Over a range of doping from  $x \sim 0.2-0.5$  the manganites exhibit sharp transitions between a high-temperature paramagnetic semiconductorlike phase to a low-temperature ferromagnetic metal.<sup>8,12</sup> Although the general form of the resistivity and magnetization is similar across different samples, the transition temperature, peak resistivity, and peak magnetoresistance appear to depend sensitively on sample processing conditions and doping level, with larger magnetoresistances being observed for samples with lower transition temperatures within the same parent system.<sup>12-14</sup> While attention has focused on the very large magnetoresistance (MR) obtainable for materials with low ( $\sim 100$  K) transition temperatures, relatively little work has been done on single-crystal samples.<sup>1,15,16</sup> In particular, the  $T \rightarrow 0$  behavior of the MR in a single-crystal sample had not been measured and the variation in the field dependence of the resistivity above and below the transition remains unexplained. We have synthesized high-quality single crystals of  $\text{La}_{0.6}\text{Pb}_{0.4}\text{MnO}_{3-\delta}$  and  $\text{Nd}_{0.6}(\text{Sr}_{0.7}\text{Pb}_{0.3})_{0.4}\text{MnO}_{3-\delta}$  to obtain intrinsic bulk magnetotransport properties and address these unanswered questions regarding the origin of the exceptionally large magnetoresistance in these materials.

Single crystals of  $\text{La}_{0.6}\text{Pb}_{0.4}\text{MnO}_{3-\delta}$  and  $\text{Nd}_{0.6}(\text{Sr}_{0.7}\text{Pb}_{0.3})_{0.4}\text{MnO}_{3-\delta}$  were prepared using a flux method.<sup>1,17</sup> A 5:1 by weight mixture of flux

(equal weights of  $\text{PbO}$  and  $\text{PbF}_2$ ) and stoichiometric  $\text{La}_{0.67}\text{Pb}_{0.33}\text{MnO}_3$  or  $\text{Nd}_{0.67}\text{Sr}_{0.33}\text{MnO}_3$  powder (from oxide precursors) was finely ground and loaded into Pt crucibles covered with Pt lids. The Pt crucibles were then inserted into covered alumina crucibles. The loaded crucibles were heated in air from room temperature to 1700 K over 3 h, maintained at 1700 K for 16 h, and then slowly cooled to 1300 K at a rate of 2 K per hour, at which point the furnace was turned off and the samples were allowed to return to room temperature. The powder partially melts during the 1700 K soaking period. Crystals grow during the slow cooling.

Thick, shiny, rectangular parallelepiped single crystals of typical dimensions 1 mm  $\times$  1 mm  $\times$  0.3 mm were extracted from the exposed surface and from cavities within the solidified flux. Energy dispersive x-ray (EDX) spectroscopy revealed that a modest amount of  $\text{Pb}^{2+}$  ions from the flux had been introduced into the Nd-Sr-Mn-O crystals. The crystals used in this study were uniform in composition with La:Pb:Mn and Nd:Sr:Pb:Mn ratios of 0.6:0.4:1.0 and 0.6:0.28:0.12:1.0, respectively, within the accuracy of the EDX measurements. Figure 1 shows an x-ray diffraction pattern for a  $\text{Nd}_{0.6}(\text{Sr}_{0.7}\text{Pb}_{0.3})_{0.4}\text{MnO}_{3-\delta}$  single crystal. Only sharp (001) and (002) peaks are observed, demonstrating the high quality of the crystal.

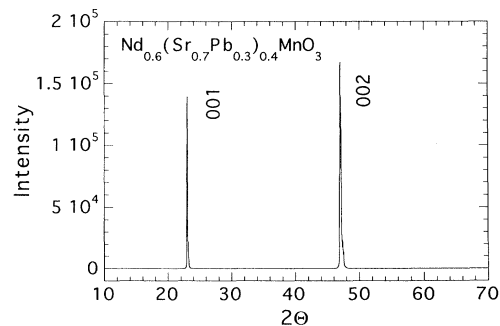


FIG. 1. X-ray diffraction pattern of a  $\text{Nd}_{0.6}(\text{Sr}_{0.7}\text{Pb}_{0.3})_{0.4}\text{MnO}_{3-\delta}$  single crystal. The reflections ( $hkl$ ) are indexed as shown.

The x-ray results show that the crystal has cubic symmetry with a lattice constant of 3.86 Å.

The resistivity was measured using a conventional dc four probe technique over temperatures from 4 to 350 K and fields ranging up to 7 T. Magnetic susceptibility of the crystals was measured with a commercial superconducting quantum interference device magnetometer. Figure 2 shows the temperature dependence of the resistivity for a  $\text{Nd}_{0.6}(\text{Sr}_{0.7}\text{Pb}_{0.3})_{0.4}\text{MnO}_{3-\delta}$  single crystal at 0 and 6 T. The temperature dependence of the magnetoresistance, defined as  $\frac{R(6\text{ T})-R(0\text{ T})}{R(0\text{ T})}$ , is also plotted, showing the characteristic negative MR peak near the resistivity transition. For zero applied field the resistivity reaches a maximum at roughly 256 K; below this temperature the resistivity falls rapidly while the magnetization rises to its saturation value. An applied field of 6 T raises the transition temperature and broadens and suppresses the resistivity peak, yielding a large magnetoresistance over a wide temperature range. The inset shows the temperature dependence of the magnetization at 1 T for the same crystal, clearly showing the magnetic transition associated with the resistive transition and the peak in the magnetoresistance. The saturation magnetization is close to the theoretical value of 83 emu/g for the relevant concentrations of  $\text{Mn}^{3+}$  and  $\text{Mn}^{4+}$ . The spontaneous magnetization and hysteresis are extremely small, providing additional evidence of the high quality and purity of the single-crystal samples.

Figure 3 shows the temperature-dependent resistivity of a  $\text{La}_{0.6}\text{Pb}_{0.4}\text{MnO}_{3-\delta}$  single crystal at 0 and 6 T, the inset showing the magnetization as a function of temperature at 1 T. The resistivity at zero field peaks at 355 K, and the maximum MR of  $-64\%$  occurs above room temperature at 314 K. The large, broad MR peak above room temperature holds promise for exploitation in device applications. Keeping in mind the general trend of increasing magnitude of MR with decreasing transition temperature, these lead-doped manganite perovskites promise further increases in MR upon adjustment of doping level and processing conditions.

At low temperatures virtually no magnetoresistance

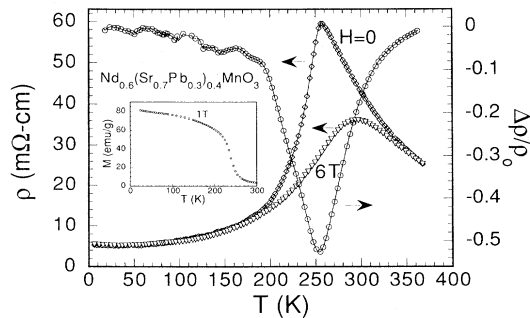


FIG. 2. Temperature dependence of the electrical resistivity and magnetoresistance  $\frac{R(6\text{ T})-R(0\text{ T})}{R(0\text{ T})}$  for a single crystal of  $\text{Nd}_{0.6}(\text{Sr}_{0.7}\text{Pb}_{0.3})_{0.4}\text{MnO}_{3-\delta}$ . The inset shows the magnetization  $M$  versus temperature at  $H = 1\text{ T}$  for the same crystal.

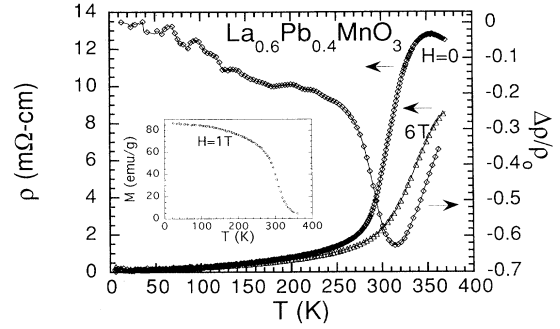


FIG. 3. Temperature dependence of the electrical resistivity and magnetoresistance  $\frac{R(6\text{ T})-R(0\text{ T})}{R(0\text{ T})}$  for a single crystal of  $\text{La}_{0.6}\text{Pb}_{0.4}\text{MnO}_{3-\delta}$ . The inset shows the magnetization  $M$  versus temperature for an applied field of 1 T for the same crystal.

is observed for either sample, in contrast to the results obtained previously for polycrystalline materials.<sup>12,13</sup> As  $T \rightarrow 0$  spin fluctuations are frozen out within each magnetic domain, arguing against the possibility of intrinsic MR at  $T=0$ . The finite MR obtained for polycrystalline samples at  $T=0$  most likely results from scattering at grain boundaries or possibly defects. Domain wall scattering is an unlikely source of the finite  $T=0$  MR in polycrystalline samples since our single crystals, which also contain domain walls, have zero MR as  $T \rightarrow 0$ . Nonmagnetoresistive grain boundaries have been proposed as the cause of the smaller MR observed in polycrystalline samples as compared to epitaxial thin films.<sup>5</sup> However, the overall magnitude of the MR in our single crystal samples is comparable to polycrystalline materials, indicating that the absence of grain boundaries is not the critical ingredient in obtaining the largest MR.

Figure 4(a) shows the field-dependent resistivity for a  $\text{La}_{0.6}\text{Pb}_{0.4}\text{MnO}_{3-\delta}$  crystal normalized by the values at zero applied field. Below the transition temperature  $T_C$  the resistivity decreases linearly with field at moderate fields, eventually following a roughly exponential behavior. The resistivity above  $T_C$  is quadratic in the magnetic field over a broad range of field. This behavior can be interpreted within a generalized two-component polaron model in which the difference in relative concentration of charge carriers with spins parallel versus antiparallel to the field gives rise to the differing behaviors of  $\rho(H)$  above and below  $T_C$ .

The preconditions for polaron formation, namely, large electron-lattice coupling and low electronic hopping rates, appear to be satisfied for the manganite perovskites.<sup>18</sup> Consider a model with two flavors of charge carriers, spin up and spin down electrons, which act as polarons with spin-dependent binding energies  $E_b(c_\uparrow)$  and  $E_b(c_\downarrow)$ , respectively, where  $c_\uparrow$  ( $c_\downarrow$ ) is the fraction of spin-up (-down) electrons. We obtain a polaron conductivity<sup>19</sup>

$$\sigma \propto \frac{1}{T} \left( c_\uparrow e^{-\frac{E_b(c_\uparrow)}{T}} + c_\downarrow e^{-\frac{E_b(c_\downarrow)}{T}} \right). \quad (1)$$

Expressing the conductivity in terms of the reduced mag-

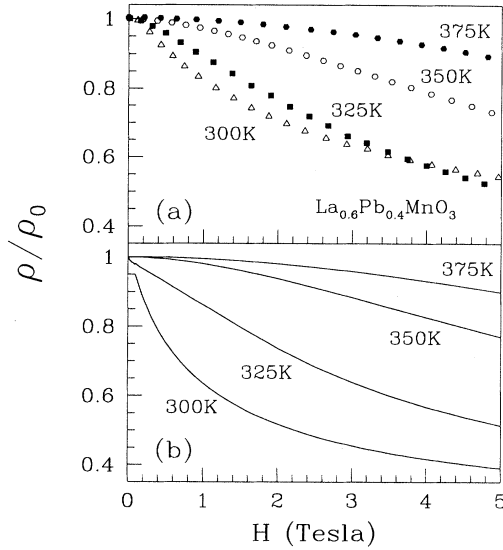


FIG. 4. (a) Magnetic field dependence of the resistivity for the same  $\text{La}_{0.6}\text{Pb}_{0.4}\text{MnO}_{3-\delta}$  crystal as in Fig. 3. The resistivities are normalized by the respective zero-field values. (b) Theoretical fit for the two-component lattice polaron model discussed in the text.

netization of the conduction electrons defined as  $m = c_{\uparrow} - c_{\downarrow}$  yields

$$\sigma \propto \frac{1}{T} \left[ (1+m) e^{-\frac{E_b(\frac{1}{2}(1+m))}{T}} + (1-m) e^{-\frac{E_b(\frac{1}{2}(1-m))}{T}} \right], \quad (2)$$

which can be expressed in the general form

$$\sigma \propto \frac{1}{T} (f(m) + f(-m)). \quad (3)$$

$E_B$  is expected to be a smooth function of  $m$ , particularly for  $m$  small, so that we can make a Taylor expansion of  $f(m)$  for  $|m| \ll 1$ . The linear terms cancel and  $\sigma(M)$  is well approximated by the constant and quadratic terms. Since the magnetization for  $m \ll 1$  is linear in the applied field, the resistivity is quadratic in the magnetic field whenever the magnetization is small. At low to moderate fields above the transition (i.e., the regime in which  $m \ll 1$ ) we observe this quadratic dependence of resistivity on field.<sup>20</sup> Note that this behavior is general to a differentiable two-component model irrespective of the detailed physics.

At temperatures below the transition the conductivity in the polaron model is dominated by the majority-spin carriers. Sufficiently close to the transition Eq. (2) should still be valid (at lower temperatures the majority-spin polarons unbind and hence other scattering processes dominate). The dominant term in the field-dependent conductivity then arises from the majority spin component, yielding the near-exponential behavior of  $\rho(H)$  observed in Fig. 4(a) for  $T < T_C$ .

Within a polaron model of GMR the transition from semiconductorlike to metallic behavior results from an unbinding of the polarons in the magnetically ordered state. A small lattice polaron forms when the residence time of an itinerant electron on a given lattice site becomes comparable to a characteristic optical phonon frequency; for sufficiently slow hopping rates and sufficiently large electron-phonon coupling the system becomes unstable to the localization of charge carriers within small lattice distortions. Disorder in the electronic hopping rates may further encourage polaron formation through initial nucleation at the most favorable sites followed by preferential polaron formation at adjacent sites.<sup>21</sup> Relatively small changes in electronic hopping rate can drive a system through an instability into a polaronic phase.

Within double exchange theory the hopping of electrons between sites of antialigned ionic spin is suppressed by Hund's rule.<sup>9,10</sup> This suppression of electronic hopping by the spin disorder in the high-temperature paramagnetic phase may be sufficient to cause polaron formation. The alignment of the spins upon cooling through the magnetic transition may then reduce the residency times of the majority-spin carriers sufficiently to unbind the majority-spin polarons. A polaronic instability accompanies the spin-ordering transition. We emphasize that within double exchange alone the change in electronic hopping rates at the magnetic transition produces only a small change in resistivity<sup>15,18</sup>—it is the transition to a polaronic state which can account for the large observed change in resistivity.

A slightly more detailed picture of the two-component polaron model can be obtained by taking the simplest possible form for  $E_b$ , namely,  $E_b(c_{\uparrow}) = \gamma(1 - c_{\uparrow})$ , with  $\gamma$  an arbitrary constant. This expression may be considered a lowest order Taylor expansion for the true  $E_b(c_{\uparrow})$ , wherein the polarons are completely unbound in the spin-ordered state. We assume that the fractional spin alignment of the conduction electrons is accurately reflected by the total magnetization, localized electrons included, so that we may use the experimental magnetization curves to determine the fractional spin concentrations.<sup>22</sup> Choosing  $\gamma = 900$  K, we obtain the normalized resistivity versus field curves shown in Fig. 4(b). The semiquantitative agreement with experiment (for only one free parameter beside the overall scale) suggests that perhaps this model has captured the essential physics.

Magnetopolarons would be expected to be subject to the same physical effects of changes in hopping amplitudes as lattice polarons. A magnetopolaron model contains an additional source of unbinding in that the scope for a local spin distortion decreases strongly as the spins become ordered. Although a detailed analysis of conductivity within a magnetopolaron model would be more involved than the simple treatment given here for lattice polarons, the qualitative behavior of the resistivity near the transition should be similar. We note, however, that doubts exist as to whether the effective carrier-spin interaction within double exchange is strong enough to produce self-trapped magnetopolarons.<sup>18</sup>

In summary, analysis of single crystals of two families

of manganite perovskites has provided important information pertaining to the mechanism of the giant magnetoresistance in these materials. The magnetoresistance of single-crystal manganite perovskites vanishes as  $T \rightarrow 0$ , suggesting that the finite zero-temperature MR observed in polycrystalline samples is a grain boundary effect. One previously proposed explanation for the enormous variations in MR among thin film samples had been that nonmagnetoresistive grain boundaries short out the magnetoresistive regions in the lower-MR samples. The moderate size of the MR in our single crystals suggests that a lack of grain boundaries is not a sufficient condition for extremely large MR. The quadratic dependence of the resistivity on field above the transition is shown to be a

general consequence of a two-component model of electronic conduction. Further investigations of a detailed microscopic mechanism for polaron formation would shed light on the possible relevance of a two-component polaron model for the giant magnetoresistance of these materials.

V.H.C. acknowledges useful discussions with D. R. Penn. This work was supported by National Science Foundation Grant Nos. DMR-9120269 and DMR-9017254 and by the Director, Office of Energy Research, Office of Basic Energy Sciences, Materials Sciences Division of the U.S. Department of Energy under Contract No. DE-AC03-76SF00098.

- 
- <sup>1</sup> R. M. Kusters, J. Singleton, D. A. Keen, R. McGreevy, and W. Hayes, *Physica B* **155**, 362 (1989).
- <sup>2</sup> G. C. Xiong, Q. Li, H. L. Ju, S. N. Mao, L. Senapati, X. X. Xi, R. L. Greene, and T. Venkatesan, *Appl. Phys. Lett.* **66**, 1427 (1995).
- <sup>3</sup> R. von Helmolt, J. Wecker, B. Holzapfel, L. Schultz, and K. Samwer, *Phys. Rev. Lett.* **71**, 2331 (1993).
- <sup>4</sup> H. L. Ju, C. Kwon, Q. Li, R. L. Green, and T. Venkatesan, *Appl. Phys. Lett.* **65**, 2108 (1994).
- <sup>5</sup> S. Jin, T. H. Tiefel, M. McCormack, R. A. Fastnacht, R. Ramesh, and L. H. Chen, *Science* **264**, 413 (1994).
- <sup>6</sup> K. I. Chahara, T. Ohno, M. Kasai, and Y. Kozono, *Appl. Phys. Lett.* **63**, 1990 (1993).
- <sup>7</sup> S. S. Manoharan, N. Y. Vasanthacharya, M. S. Hegde, K. M. Satyalakshmi, V. Prasad, and S. V. Subramanyam, *J. Appl. Phys.* **76**, 3923 (1994).
- <sup>8</sup> G. H. Jonker and J. H. Van Santen, *Physica* **16**, 337 (1950).
- <sup>9</sup> C. Zener, *Phys. Rev.* **82**, 403 (1951).
- <sup>10</sup> P.-G. deGennes, *Phys. Rev.* **118**, 141 (1960).
- <sup>11</sup> E. O. Wollan and W. C. Koehler, *Phys. Rev.* **100**, 545 (1955).
- <sup>12</sup> P. Schiffer, A. P. Ramirez, W. Bao, and S.-W. Cheong (unpublished).
- <sup>13</sup> Y. X. Jia, L. Lu, K. Khazeni, D. Yen, C. S. Lee, and A. Zettl, *Solid State Commun.* **94**, 917 (1995).
- <sup>14</sup> M. F. Hundley, M. Hawley, R. H. Heffner, Q. X. Jia, J. J. Neumeier, J. Tesmer, J. D. Thompson, and X. D. Wu (unpublished).
- <sup>15</sup> C. W. Searle and S. T. Wang, *Can. J. Phys.* **48**, 2023 (1970).
- <sup>16</sup> J. Z. Liu (unpublished).
- <sup>17</sup> D. Elwell and H. J. Scheel, *Crystal Growth from High-Temperature Solutions* (Academic, New York, 1975).
- <sup>18</sup> A. J. Millis, P. B. Littlewood, and B. I. Shraiman, *Phys. Rev. Lett.* **74**, 5144 (1995).
- <sup>19</sup> N. F. Mott and E. A. Davis, *Electronic Processes in Non-crystalline Materials* (Clarendon, Oxford, 1979).
- <sup>20</sup> The sign of the quadratic term in  $\rho = a + bm^2$  is negative so long as the field dependence of the binding energy around  $m \approx 0$  is dominated by the term linear in  $H$ .
- <sup>21</sup> D. Emin and M.-N. Bussac, *Phys. Rev. B* **49**, 14 290 (1994).
- <sup>22</sup> The experimental magnetization versus magnetic field curves for temperatures below the transition were extrapolated to zero field using a mean field theory in order to remove the dependence of the magnetization on domain realignment at small fields. A detailed treatment of this domain alignment might be expected to yield a very small region of quadratic behavior near  $H = 0$  for  $T < T_C$ .